

First evidence for a *Vibrio* strain pathogenic to *Mytilus edulis* altering hemocyte immune capacities

Ben Cheikh Yosra ¹, Travers Marie-Agnes ², Morga Benjamin ², Godfrin Yoann ², Rioult Damien ³, Le Foll Frank ^{1,*}

¹ Laboratory of Ecotoxicology- Aquatic Environments, UMR-I 02, SEBIO, University of Le Havre, F-76063, Le Havre Cedex, France

² Ifremer, SG2M-LGPMM, Laboratoire de Génétique et Pathologie des Mollusques Marins, Avenue de Mus de Loup, 17390, La Tremblade, France

³ Laboratory of Ecotoxicology- Aquatic Environments, UMR-I 02, SEBIO, University of Reims Champagne Ardenne, Campus Moulin de la House, F-51100, Reims, France

* Corresponding author : Frank Le Foll, email address : frank.lefoll@univ-lehavre.fr

Abstract :

Bacterial isolates were obtained from mortality events affecting *Mytilus edulis* and reported by professionals in 2010–2013 or from mussel microflora. Experimental infections allowed the selection of two isolates affiliated to *Vibrio splendidus/Vibrio hemicentroti* type strains: a virulent 10/068 1T1 (76.6% and 90% mortalities in 24 h and 96 h) and an innocuous 12/056 M24T1 (0% and 23.3% in 24 h and 96 h). These two strains were GFP-tagged and validated for their growth characteristics and virulence as genuine models for exposure. Then, host cellular immune responses to the microbial invaders were assessed. In the presence of the virulent strain, hemocyte motility was instantaneously enhanced but markedly slowed down after 2 h exposure. By contrast, hemocyte velocity increased in the presence of the innocuous 12/056 M24T1. At the same time interval, 10/068 1T1 invaded hemocytes and was more rapidly internalized than the innocuous strain. Extracellular products (ECPs) prepared from 10/068 1T1 cultures significantly inhibited phagocytic activity while 12/056 M24T1 ECPs had no effect. Furthermore, the pathogenic strain and its ECPs inhibited oxidative burst unlike 12/056 M24T1 strain/ECPs which enhanced ROS production. Taken together, our results suggest that the mussel pathogen 10/068 1T1 may escape immune response by altering hemocytes functions.

Highlights

► Isolation of a *Vibrio* strain pathogenic to the blue mussel. ► Two differentially virulent *Vibrio* strains were GFP-labeled. ► The virulent strain altered hemocyte motility and quenched ROS production. ► ECPs from the virulent strain inhibited bead phagocytosis and ROS production. ► The virulent strain was rapidly internalized in hemocytes.

Keywords : innate immunity, molluscs, cell-mediated immune response, bacterial infections, green fluorescent protein

57

58 1. Introduction

59 Shellfish farms have been impacted by bacterial infectious diseases for many years,
60 inducing repeated episodes of mortality and consequently important economic loss. The most
61 common causative agent is represented by members of the genus *Vibrio* capable of infecting
62 oysters, abalone, clams, and scallops at different life stages: larval, juvenile and adult (Beaz-
63 Hidalgo et al., 2010a; Travers et al., 2015). Among bivalve species and until recently, mussels
64 were not massively affected by bacterial pathogens (Gestal et al., 2008; Watermann et al.,
65 2008). This relative resistance has been related to a robust innate immunity able to prevent
66 efficiently bacteria infestation (Balbi et al., 2013; Ciacci et al., 2010; Tanguy et al., 2013).
67 Nevertheless, since 2010, abnormal mortality events were also reported for farmed blue
68 mussels (juveniles and adults) in France (Bechemin et al., 2014; Guichard et al., 2011).
69 During this period, different *Vibrio* strains were isolated from moribund animals. Primary
70 investigations on recent mortality events suggest that these episodes could be accounted for
71 by multiple reasons, including a combination of particular environmental conditions together
72 with biological factors (Bechemin et al., 2014).

73 Host-pathogen interactions implicate multiple processes initiated both by the pathogen, as
74 a strategy to survive, and the host in an attempt to eliminate the invader (Gestal et al., 2008).
75 Whilst *Vibrio* virulence has been frequently associated to secretion of extracellular products
76 (Labreuche et al., 2010, 2006), lesions and infection kinetics remain poorly understood
77 because of the diversity of bacteria and the number of hosts and age classes they can infect
78 (Travers et al., 2015). The study of immune systems may help to understand responses of
79 hosts facing invaders. As other bivalves, mussels are endowed of exclusive innate immune
80 responses carried out by circulating hemocytes and soluble hemolymph factors (Canesi et al.,
81 2002).

82 *Mytilus edulis* immunocytes form an heterogeneous cell population. They can be classified
83 into 3 main groups of hemocytes, small semi-granular basophils, agranular hyalinocytes and
84 more complex granulocytes (Le Foll et al., 2010). These cells are involved in various
85 physiological functions but their key role consist in internal defense since they are able to
86 recognize, bind, and phagocytize microbes. Phagocytosis is the primary mechanism for
87 bacterial killing and elimination of foreign particles in these organisms. It can be divided into
88 several stages, including chemotaxis, recognition, adhesion, endocytosis and destruction
89 (Gosling, 2015). Mussel hemocytes are motile, they migrate to infected sites following the

90 detection of foreign materials (Donaghy et al., 2009), leading to pathogens recognition and
91 adhesion. Internalization is the key stage of microbicidal activity. During this process,
92 sophisticated cascades of reactions involving multiple molecular partners take place. As a
93 consequence, phagocytes produce free radicals derived from oxygen and nitrogen, highly
94 toxic to the ingested pathogens, and release lysosomal enzymes as well as antimicrobial
95 peptides (Canesi et al., 2002; Mitta et al., 2000).

96 Nevertheless, the immune response is sometimes insufficient to defeat microbial
97 aggressions. Bacteria can be pathogenic to host, having the ability to cause diseases and death.
98 The degree of pathogenicity corresponds to virulence, a phenotype intimately dependent on
99 host-pathogen interactions (Casadevall and Pirofski, 2009; Steinhaus and Martignoni, 1970).
100 Experimental infections of *Mytilus sp.* and *in vitro* studies using hemocytes co-incubated with
101 various *Vibrios* have generated data describing systemic, cellular and molecular responses of
102 mussels to bacteria (Ciacci et al., 2010, 2009; Costa et al., 2009; Parisi et al., 2008; Tanguy et
103 al., 2013). However, bacterial strains used in these studies, like *V. splendidus* LGP32 or *V.*
104 *aestuarianus* 01/132, are pathogens of the pacific oyster *Crassostrea gigas* with, by contrast,
105 no characterized virulence towards the blue mussel. Thus, it should be considered that, up to
106 now, results reported from bacterial challenges of *Mytilus sp.* immunity were obtained in a
107 context of low virulence.

108 In this work, we evaluated the virulence of bacterial isolates in the adult blue mussel by
109 carrying out experimental infections and characterizing hemocyte responses. Experimental
110 infections led to the selection of two isolates affiliated to *V. splendidus/V. hemicentroti*
111 groups: a virulent and an innocuous strain. Corresponding GFP-tagged *Vibrio* strains were
112 constructed and validated to be used in flow cytometry and fluorescence microscopy.
113 Responses of blue mussel hemocytes exposed to virulent/non virulent *Vibrio* strains or to their
114 extracellular products during different phases of phagocytosis were examined.

115 **2. Material and methods**

116 **2.1. Mussel collection**

117 Adult mussels, *M. edulis* with shell length ranging from 4 to 5 cm, were collected on the
118 intertidal rocky shore of Yport (0°18'52"E:49°44'30"N, France) between December 2013 and
119 December 2015, immediately transported to the laboratory and placed in a temperature-
120 controlled (10°C) aerated Biotop Nano Cube 60 seawater tank (Sera, Heinsberg, Germany) ,
121 equipped with mechanical and activated biological filtering. The animals were fed with algae
122 (*Isochrysis galbana*) and maintained in these conditions for at least one week before use.

123 2.2. Bacterial strains

124 2.2.1. Isolation from mussels (Laboratoire National de Référence, LNR, La Tremblade)

125 Strains used in this study are described in **Error! Reference source not found..** Bacteria were
126 isolated from mussel mortality events reported by professionals (French national surveillance
127 network REPAMO) in 2010 and 2013, or from mussel microflora in absence of mortality in
128 the context of Bivalife European project in 2011 and 2012. Briefly, crushed tissues were
129 homogenized in 100 µl of Sterile Artificial Sea Water (SASW : 2.3 % (w/v) NaCl, 20 mM
130 KCl, 5 mM MgSO₄, 2 mM CaCl₂) with a sterile pellet-pestle (Sigma) for 1 minute on average.
131 Samples diluted 100x and 1000x in SASW were plated on Zobell agar (0.4% peptone, 0.1%
132 yeast extract, 0.01% ferric citrate and 1.5 % agar in SASW, pH 7.6) and the predominant
133 bacteria were isolated after 48h at 20°C. Pure cultures of bacterial strains were conserved
134 frozen at -80°C in Zobell broth with glycerol 15%.

135 2.2.2. Genetic characterization: *gyrB* sequencing

136 Total DNA from a log-phase culture was extracted from cultured *Vibrio* by boiling in 100
137 µl of ultrapure water (Saulnier et al., 2009). The *gyrB* (gyrase B) gene was amplified using the
138 universal bacterial primer pairs (*gyrB*274F GAAGTTATCATGACGGTACTTC and
139 *gyrB*1171R CCTTTACGACGAGTCATTTTC) and the methods previously described
140 (Thompson et al., 2005). Amplicons with the expected size were purified using a Microcon
141 PCR filter kit (Millipore). Purified PCR products were mixed (final volume 10 µl) with 0.4 µl
142 ABI Prism Big Dye Terminator ready reaction mix (Applied Biosystems®) and 0.75 µM of
143 primer. Cycle sequencing reactions were performed using a Gene Amp PCR System 2700
144 (Applied Biosystems®) and following the manufacturer's instructions. Separation of the DNA
145 fragments was carried out in an ABI PRISM 3130 XL Genetic Analyzer (Applied
146 Biosystems).

147 Sequences were aligned using ClustalW (<http://www.ebi.ac.uk/Tools/msa/clustalw2/>) and
148 BioEdit software (<http://www.mbio.ncsu.edu/bioedit/bioedit.html>.) Phylogenetic tree was
149 built using Mega6 (<http://www.megasoftware.net/mega6/mega.html>.) The tree was drawn
150 using the Neighbor-Joining method with the Kimura two-parameter model (Saitou and Nei,
151 1987). Reliability of topologies was assessed by the bootstrap method (Felsenstein, 1985)
152 with 1000 replicates. The Genbank accession numbers gene sequences obtained in this study
153 or already published in GenBank are presented in **Error! Reference source not found..**

154 2.2.3. Characterization of virulence by *in vivo* injections

155 Bacteria were grown overnight in Marine broth or Luria Bertani NaCl 20 g.L⁻¹ at 22°C
156 with constant agitation (80 rpm). Cells were washed twice with filtered sterile seawater
157 (FSSW) and centrifuged at 1200 g for 10 min. The supernatant was discarded and the
158 resulting pellet resuspended in FSSW to obtain an OD_{600nm} of 1. Mussels were anesthetized
159 for 2–3 h at 20°C in a magnesium chloride solution (MgCl₂, Sigma Aldrich) at a final
160 concentration of 50 g.L⁻¹ (1/4: v/v seawater/freshwater) and under aeration. Subsequently, a
161 volume of 100 µl of bacterial suspension was injected into the posterior adductor muscle. A
162 group of mussel was injected with FSSW to serve as negative controls. After injection, the
163 animals were transferred to tanks (3 replicate tanks, 10 mussels per tank) filled with 2L of
164 UV-treated and filtered seawater supplemented with 50 ml of phytoplankton and maintained
165 under static conditions at 20°C with aeration. Mortality was monitored each day over a four
166 day period. Animals were considered to be dead when the valves did not close following
167 stimulation. Newly dead mussels were removed from the tanks.

168 2.2.4. GFP-tagging by triparental mating

169 The pVSV102 plasmid (Dunn et al., 2006) carrying GFP/ kanamycin-resistance expression
170 cassette was transferred from *E. coli* to *Vibrio* strains (10/068 1T1, 12/056 M24T1) by
171 triparental mating (Stabb and Ruby, 2002) using the conjugative helper strain CC118 λpir as
172 described by Dunn et al. (2006). Donor, helper and receptor cells were grown overnight to the
173 stationary phase in Luria Bertani (LB) (*E. coli* strains) and LBS [LB complemented with salt,
174 NaCl 20 g.L⁻¹ (f.c.), for *Vibrio* strains] with addition of 40 µg.mL⁻¹ kanamycin for DH5α-
175 pVSV102. 100 µL of each culture was combined in a microfuge tube, washed in LBS without
176 antibiotics and centrifuged at 1200 g for 10 min. The resulting pellet was suspended into 10
177 µL of LBS and dropped on a fresh LBS agar plate and then incubated for 16 hours at 28°C.
178 The bacterial spot was suspended in 800 µL of LBS, serially diluted, plated on LBS plates
179 containing 100 µg.L⁻¹ kanamycin and incubated at 18°C. Donor bacteria were counter-
180 selected by growing at 18°C, whereas the helper strain and the acceptor strain, which did not
181 receive conjugative, plasmids were killed by the antibiotic selection. Therefore, clones were
182 isolated by inoculation into new LBS antibiotic plates and green fluorescent were verified by
183 epifluorescence microscopy.

184

185 2.2.5. Validation of GFP-tagged strains

186 GFP expression conservation: To ensure plasmid conservation, fluorescent bacteria strains
187 were grown overnight in LBS 100 $\mu\text{g.L}^{-1}$ kanamycin at 22°C. This culture was diluted in LBS
188 without antibiotics and grown at 22°C overnight. Every day, a new culture was started with an
189 aliquot of the previous day's culture, which was analyzed by flow cytometry, after dilution.

190 Growth curves: Parental bacterial strains and GFP-tagged strains were cultivated in LBS at
191 22°C with constant shaking at 80 rpm. At regular intervals, the bacterial concentrations in the
192 cultures were evaluated spectrophotometrically at an optical density (OD) of 600 nm.

193 In vivo injection: To compare virulence between parental and derivative fluorescent strains,
194 GFP-tagged strains were injected intramuscularly into mussels according to the protocol
195 described above for parental strains.

196 2.3. Contact with hemocytes

197 2.3.1. Haemolymph collection

198 Haemolymph was withdrawn from the posterior adductor muscle sinus, by gentle
199 aspiration with a 1 mL syringe equipped with a 22G needle. Quality of samples was
200 systematically checked by microscopic observation before using in bioassays.

201 2.3.2. Preparation of bacteria and their extracellular products

202 For *in vitro* experiments, two *Vibrio* strains were used: 10/068 1T1 and 12/056 M24T1
203 (parental or GFP-tagged). Bacteria were cultivated overnight in Marine broth or Luria Bertani
204 NaCl 20 g.L^{-1} at 22°C, centrifuged at 3000 g for 10 min. Supernatants were filtered (0.22 μm)
205 and conserved at -20°C until use and bacteria were diluted in sterile physiological water
206 (NaCl 9 g.L^{-1}) at 10^8 cfu.ml⁻¹ for immediate utilization.

207 2.3.3. Motility

208 Hemocyte motility was assessed via live-cell nuclei tracking. The protocol was adapted
209 from Rioult et al. (2013). Briefly cells exposed to bacteria (10^8 cfu.ml⁻¹) or in marine
210 physiological saline solution (MPSS) pH 7.8, 0.2 μm filtered (Rioult et al., 2014) for the
211 control were incubated with 5 μM of the nuclei-specific fluorescent probe Hoechst 33342 for
212 15 minutes at 15°C. A culture dish was placed on the stage of a TE-2000 inverted microscope
213 (Nikon, Champigny-sur-Marne, France) equipped for epifluorescence excitation (HBO arc
214 lamp with 377/50 nm bandpath filter) and time-lapse imaging. A Peltier temperature
215 controller (PDMI-2 and TC-202A; Harvard Apparatus, Holliston, MA) keeps preparation at

216 15°C for extended live cell imaging. Wild-field epifluorescence time-lapse imaging was
217 performed with a x10 objective (numerical aperture 0,3). A VCM-D1 shutter (Uniblitz,
218 Vincent Associates, NY) was added in the illumination pathway to cut off the excitation light
219 between two image recordings. Camera and shutter were controlled by Metamorph
220 (Molecular Device, Sunnyvale, CA) as acquisition software. A CCD Coolsnap EZ camera
221 (Photometrics, Tucson, AZ) captured 12-bit digital of 1392×1040 pixels greyscale images
222 every 30 s for 2 hours (409 nm long path emission filter). Camera and software were
223 calibrated to express distance in microns. Time-series image stacks were imported into
224 Metamorph Analysis software. The track Objects application (available with Multi-
225 Dimensional Motion Analysis option) was started. Typically, for each biological replicate, 20
226 nuclei were randomly chosen to be tracked. Extracted data were transferred to a spreadsheet
227 and, for each cell, the mean distance travelled during 30 seconds was calculated and
228 multiplied by 2 to express velocity in $\mu\text{m}\cdot\text{min}^{-1}$.

229 **2.3.4. Phagocytosis assay**

230 The phagocytic ability of hemocytes was determined by flow cytometry using fluorescent
231 beads or GFP tagged bacteria. Internalization of beads or bacteria was verified by microscopic
232 observation.

233 The protocol was adapted from Costa et al. (2009) with some modifications. Briefly,
234 fluospheres (Fluosphere Carboxylate-Modified Microspheres, 2.00 μm , yellow-Green, Life
235 technologies) were added to haemolymph to generate minimally a 10:1 bead to hemocyte
236 ratio and cells were incubated for 2, 4 and 6 hours at 15°C in the dark. The effect of bacterial
237 extracellular products (ECPs) was tested by mixing 100 μl of ECPs to cell suspension one
238 hour before adding beads. After incubation, supernatants were gently aspirated and attached
239 cells were removed by adding cold Alsever's solution (300 mM NaCl, 100 mM Glucose, 30
240 mM sodium Citrate, 26 mM citric acid, 10 mM EDTA, pH 5.4) and analyzed by Beckman
241 Coulter flow cytometer. Phagocytosis was defined as cell internalization of 3 beads or more.

242 The capacity to phagocyte bacteria was also evaluated. Cells were exposed to GFP-tagged
243 *Vibrio* strains at 10:1 ratio (bacteria:cell) for 2, 4 and 6 hours at 15°C in the dark. Before
244 analysis on flow cytometry, propidium iodide was added to quantify the percentage of viable
245 cells.

246 **2.3.5. ROS production**

247 Crude haemolymph was placed into individual wells of 24-well tissue-culture plates
248 (Greiner) and cells allowed to adhere for 15 minutes at 15 °C. The haemolymph was removed
249 and replaced with 400 µl MPSS (0.2 µm filtered) alone for the control or containing 0.2 µM
250 phorbol 12-myristate 13-acetate (PMA, Sigma) or 100 µl of ECPs or heat killed bacteria (15
251 min at 100°C). For *Vibrio* challenges, 400 µl of bacterial suspension diluted in physiological
252 water at 10^8 cfu.ml⁻¹ were added to hemocytes. After two hours of incubation at 15°C, CM-
253 H₂DCFDA at 0.2 µM f.c. was added in each well and plates were incubated 30 minutes at
254 15°C in the dark. Fluorescence was analyzed on flow cytometer (Beckman Coulter).

255 2.4. Statistical analyses

256 Statistical analysis was performed by using SigmaPlot 12 (Systat Software Inc., Chicago,
257 IL). Replicates were averaged and the values were tested for normality (Shapiro-Wilk) and
258 paired comparisons were performed by Student's t-tests or by Mann-Whitney rank sum tests
259 in case of unequal variance. Statistical significance was accepted for * $p < 0.05$, ** $p < 0.01$ or
260 *** $p < 0.001$

261 3. Results

262 3.1. Bacteria pathogenicity and genetic characterization

263 Bacterial strains were isolated from *M. edulis* during mortalities events reported by
264 professionals or from mussel microflora in absence of mortalities (**Error! Reference source not
265 found.**). Fifteen strains of *Vibrio* isolates were tested at OD₆₀₀=1 for their pathogenicity
266 toward mussels by experimental infection (Figure 1). First mortalities appears 24 hours post-
267 injection and were comprised between 0 % and 76,6 % indicating different degrees of
268 virulence between bacteria. The most virulent strain was 10/068 1T1 and caused respectively
269 $76,6 \pm 8\%$ and $90 \pm 5\%$ (n=3) mortalities after 24 and 96 hours. For 10/060 2T1 and 12/040
270 11T2 mortalities increased progressively from 5-10% after 24h to 40-47,5% after 96 hours.
271 Strains 10/058 2T1, 10/058 3T1, 11/100 M22T3, 11/148 M6T2, 12/037 M22T1, 12/037
272 M24T1, 12/037 M7T1, 12/037 M23T1, 12/056 M1T1, 12/056 M24T1, 13/026 2T3, 13/026
273 5T3 can be considered as innocuous (mortalities between 0 and 6,6 % after 24h). It is
274 important to notice that some of these strains can induce limited mortalities after 96 hours.

275 To confirm the virulence of 10/068 1T1 strain, different OD₆₀₀ doses were injected to
276 mussels (Figure 2). After 24 hours, a dose-dependent mortalities was observed ($36,6 \pm 12\%$,
277 n=3 mortalities at OD₆₀₀=0.1).

278 Phylogenetic analyses of bacteria isolates based on the housekeeping gene *gyrB* revealed
279 that the majority of isolated strains belongs to *V. Splendidus* group and can be affiliated to the
280 *V. splendidus* / *V. hemicentroti* species, or *V. lentus* / *V. atlanticus* species (Figure 3). No clear
281 correlation between phylogeny and virulence can be noticed. Conversely, few virulent strains
282 (3) were identified, all isolated from mussel mortality events (2010 and 2012), and
283 phylogenetically close to non virulent strains isolated from normal flora.

284 3.2. Validation of GFP-tagged strains

285 Two *Vibrio* strains were GFP-tagged, the virulent 10/068 1T1 and the non virulent 12/056
286 M24T1. To validate their use as genuine models for *M. edulis*, the fluorescence stability and
287 potential effects of the GFP-plasmid on bacteria growth capacities and virulence were
288 analyzed. Plasmid stability tests, determining the proportion of plasmid-bearing cells
289 remaining overtime, were conducted by culturing the GFP-labeled strains in the absence of
290 antibiotic selection. Both strains 10/068 1T1 and 12/056 M24T1 showed a high stability of
291 GFP encoding plasmid after 14 passages in a non-selective culture (Figure 4a). Bacterial
292 physiology and phenotype after GFP-tagging were also studied. No obvious difference was
293 noticed in growth characteristics (Figure 4b) and colony size or aspect when plated on LBS
294 (not shown). Furthermore, bacteria virulence did not change after transformation, both
295 parental and GFP-tagged 10/068 1T1 strains leading to 90% mussel mortality in 4 days while
296 parental and labeled 12/056 M24T1 strains caused in this experiment respectively 20% and
297 23% mortalities (Figure 4c).

298 3.3. Hemocyte motility

299 Hemocyte migration was followed *in vitro* by nuclei tracking during 2h with a recording
300 rate of 1 image/30 sec. Off-line tracking was carried out on a set of 20 nuclei selected
301 randomly in the microscopic field. In control conditions, velocity was stable with values of
302 about 1 $\mu\text{m}/\text{min}$. In the presence of *V. splendidus*-related 10/068 1T1 in the imaging chamber,
303 cell velocities were higher, 3.3 $\mu\text{m}/\text{min}$ at the beginning of the recording, and increased after
304 30 min to reach 4,8 $\mu\text{m}/\text{min}$. Then, migration speed decreased and get closer to control
305 velocity after 2 hours of recording. In contrast, the motility of hemocytes exposed to the
306 innocuous strain 12/056 M24T1 increased progressively and exceeded 5 $\mu\text{m}/\text{min}$ at the end of
307 the recording (Figure 5a). Standard error of the mean (SEM) values followed the same
308 distribution than mean velocity (Figure 5b). These results indicate that hemocytes co-
309 incubated with *V. splendidus*-related 10/068 1T1 had transiently elevated velocities at the

310 beginning of the experiments and rapidly converged towards a reduced motility in a bell-
311 shaped time course. Conversely, 12/056 M24T1 continuously activated hemocyte speed
312 during motility recordings and provoked a dispersion of single-cell velocities.

313 **3.4. Phagocytosis assays**

314 The ability of hemocytes to engulf latex beads was investigated at different time intervals
315 (Figure 6); the percentage of cells containing 3 or more beads increased with incubation time
316 and ranged from 40% at 2h to 56% at 6h. The preincubation with 10/068 1T1 ECPs altered
317 significantly the phagocytic capacity at 2h with a decrease from 40% to 22% and also at 4h
318 and 6h ($p < 0.05$). 12/056 M24 T1 ECPs did not affect phagocytosis by comparison to control.
319 The phagocytic capacity of bacteria was evaluated by challenging hemocytes with virulent
320 and non-virulent strains at different exposure time (Figure 7). The percentage of cells
321 containing one bacterium was significantly higher for hemocytes exposed to 12/056 M24T1
322 than 10/068 1T1, and rates decreased at 6h. However, cells engulfed 2 bacteria and more were
323 significantly less important for 12/056 M24T1 than 10/068 1T1 and an increase was observed
324 after 6 h exposure. Furthermore, during phagocytosis hemocytes were viable at 95% for both
325 strains (data not shown).

326 **3.5. ROS production**

327 The capacity of *M. edulis* hemocytes to produce reactive oxygen species was investigated
328 by *in vitro* exposure to a chemical activator used as a positive control (phorbol 12-myristate
329 13-acetate, PMA) and bacterial strains (living or heat killed) or their extracellular products
330 (ECPs) (Figure 8). Immunocytes respond actively and significantly to all treatments. PMA
331 activated a respiratory burst at very low concentration ($0.2\mu\text{M}$), demonstrating that mussel
332 hemocytes are able to produce toxic radicals. Bacterial strains or corresponding ECPs also
333 induced ROS production. However, significant differences were obtained according to
334 experimental conditions. Hemocyte exposure to non virulent *Vibrio* (12/056 M24T1) or to
335 12/056 M24T1 ECPs activated ROS production at levels similar or higher than PMA,
336 respectively. Conversely, when exposed to the strain 10/068 1T1 or its ECPs, hemocytes
337 generated oxygen radicals at amounts significantly inhibited by comparison to PMA-
338 stimulated levels without any reduction of cell viability (data not shown). Heat-killed 10/068
339 1T1 did not significantly modify the response compared to PMA.

340 **4. Discussion**

341 Unlike other bivalve species, *Mytilus edulis* is not known to be particularly affected by
342 any major bacterial disease (Beaz-Hidalgo et al., 2010a; Travers et al., 2015; Watermann et
343 al., 2008). It has been suggested that mussel resistance to bacterial infection was due to the
344 presence of potent immune defense mechanisms (Balbi et al., 2013; Ciacci et al., 2010, 2009;
345 Tanguy et al., 2013). However, while many studies explored mussel immune responses
346 towards Gram + and Gram – bacteria including *Vibrios* (Costa et al., 2009; Parisi et al., 2008),
347 strain virulence for *Mytilus sp. per se* was never tested. This lack of data is all the more
348 regrettable that, since 2010, abnormal mortality events have touched farmed blue mussels
349 (juveniles and adults) in France, where different bacterial strains were isolated (Guichard et
350 al., 2011).

351 In this context, we performed 1) for a first time, an evaluation of virulence and a genetic
352 characterization of bacterial strains isolated from *Mytilus edulis*, 2) a construction and
353 validation of two stable GFP-tagged *V. splendidus*-related strains for their use in flow
354 cytometry, and 3) a description of functional activity of mussel hemocytes challenged by
355 virulent and non virulent bacteria or by their extracellular products.

356 **4.1. Pathogenicity of *V. splendidus*-related strains towards the blue mussel**

357 To evaluate virulence of isolates, experimental infection assays were carried out by
358 injecting bacteria into mussels, intramuscularly. Among the tested strains, 10/068 1T1 showed
359 a high and dose dependent degree of virulence (76.6% and 90% mortalities after 24h and 96h)
360 whereas 12/056 M24T1 was found innocuous. Phylogenetic analysis using *gyrB*, one of the
361 more polymorphic housekeeping genes used for *V. Splendidus* clade (Le Roux et al., 2004),
362 revealed the affiliation of both virulent and non virulent bacteria 10/068 1T1 and 12/056
363 M24T1 to the *V. splendidus* and *V. hemicentroti* type strains. Even if more realistic protocols
364 as immersion or cohabitation challenges are needed to confirm the pathogenic potential of this
365 strain, our injection protocol yet allows a marked differentiation of phylogenetically close
366 strains with contrasted pathotypes (76.6% of mortality induced in 24 hours vs 0%).

367 Different strains related to the *Vibrio Splendidus* clade were implicated in mortalities of
368 various bivalves, including the pacific oyster (Gay et al., 2004; Lacoste et al., 2001; Saulnier
369 et al., 2010), the atlantic scallop (Lambert et al., 1999; Nicolas et al., 1996), the carpet shell
370 clam (Beaz-Hidalgo et al., 2010b) and the greenshell mussel (Kesarcodi-Watson et al., 2009).
371 An epidemiological study of *V. splendidus* strains associated with *Crassostrea gigas*
372 mortalities demonstrated genetic diversity within this group and suggested its polyphyletic

373 nature (Le Roux et al., 2004). In fact, the *V. Splendidus* group includes 16 species, many of
374 them containing virulent and non virulent strains (for instance *V. celticus*, *V. crassostreae*, *V.*
375 *cyclitrophicus*, *V. tasmaniensis* and *V. splendidus*) (Travers et al., 2015). Concerning *M.*
376 *edulis*, we conclude that, as in other mollusk species affected by *V. splendidus*-related strains,
377 a virulent pathotype cannot be discriminated through housekeeping gene sequencing since
378 virulent strains appear phylogenetically close to innocuous ones. To define this pathotype,
379 further studies based on a large collection of strains including ecological populations (Hunt et
380 al., 2008) are needed.

381 A recent study on normal microflora, *i.e.* microflora of healthy animals, associated with *M.*
382 *galloprovincialis* reveals a high diversity of strains belonging to 5 major *V. splendidus* groups
383 (Kwan and Bolch, 2015). In accordance with these results, the majority of analyzed strains are
384 close to *V. splendidus*, *V. tasmaniensis*, *V. lentus* or *V. atlanticus*, even if we didn't find *V.*
385 *toranzoniae*-affiliated genotypes. Efforts to distinguish *V. Splendidus*-related innocuous
386 bacteria that compose natural microflora of mussel from virulent pathotypes are now
387 necessary.

388 **4.2. Construction and validation of GFP-tagged bacteria**

389 To facilitate the study of interactions between *V. splendidus*-related strains and mussel
390 hemocytes, bacteria were tagged with the Green Fluorescent Protein. Fluorescent 10/068 1T1
391 and 12/056 M24T1 strains showed a high plasmid stability. They constitute useful tools for
392 flow cytometry and epifluorescence microscopy. However, in some cases, the addition of the
393 marker gene generated changes in bacterial physiology or behavior (Aboubaker et al., 2013;
394 Allison and Sattenstall, 2007; Knodler et al., 2005). To investigate undesired virulence-
395 interfering effects of GFP expression, parental and genetic-engineered bacteria were
396 compared. For both strains, our results indicate that GFP-labeling disturbed neither growth
397 characteristics nor degrees of virulence of bacteria, thus validating the use of 10/068 1T1 and
398 12/056 M24T1 GFP expressing strains as genuine models for challenging *Mytilus edulis*.

399 **4.3. Mytilus hemocyte responses to Vibrio strains**

400 Hemocytes form the first defense line of the immune system in bivalves. Similarly to cells
401 of the vertebrate monocyte/macrophage lineage, activated hemocytes achieve pathogen
402 elimination through chemotaxis, phagocytosis and cytotoxic processes, essentially (Liu,
403 2008).

404 In an early phase of response to microbial threat, hemocytes migrate toward infected sites.
405 Herein, we explored the influence of *V. splendidus*-related strains on the motility of *Mytilus*
406 *edulis* hemocytes, by using the nuclei tracking method (Riout et al., 2013). In the absence of
407 stimulation, hemocyte velocity was stable (1 $\mu\text{m}/\text{min}$). In the presence of the innocuous strain
408 12/056 M24T1, we observe a progressive speed up of cell motility over 2 hours recordings
409 that probably corresponds to a chemoactivation. Chemotactic and chemokinetic responses
410 increase the probability of physical contact between hemocytes and invaders (Schneeweiss
411 and Renwranz, 1993), accelerating their detection and recognition. In our experiments
412 however, hemocyte exposure to virulent bacteria 10/068 1T1 triggered more complex
413 responses. The first phase lasting 30 min consists in an immediate acceleration in cell
414 migration (4,7 $\mu\text{m}/\text{min}$). Thereafter, hemocyte instantaneous velocity progressively decreased
415 to reach control values after 2 h. This deceleration may be a consequence of bacteria virulence
416 capable to alter cell migration. Only few studies evoked the mobility of bivalve hemocytes,
417 their high clumping potential and chemotactic activity towards pathogens or their extracellular
418 products (Canesi et al., 2002; Pruzzo et al., 2005; Riout et al., 2013). In blue mussels,
419 Boyden chamber assays revealed that ability of blood cells to generate both chemotactic and
420 chemokinetic reactions depends on the nature of bacteria secreted molecules (Schneeweiss
421 and Renwranz, 1993). Short-term (40 min) chemoactivation have been reported from oyster
422 hemocytes that migrate to accumulate around bacteria (Alvarez et al., 1995).

423 After migration, vertebrate as invertebrate phagocytes, on encounter with foreign objects
424 surfaces, respond by sending out finger-like pseudopods to engulf detected particles (Bayne,
425 1990). This process requires a major reorganization of cytoskeletal elements in the region of
426 the cell where phagocytosis has been triggered (Russell, 2001) and the resulting filaments
427 must be removed from the base of the forming phagosome to enable its closure (Sarantis and
428 Grinstein, 2012). In our study, we first explored the effect of 10/068 1T1 ECPs on *M. edulis*
429 hemocyte capacity to engulf latex beads.

430 After 2-hours incubations, results indicate a reduction of phagocytic activity to 22%,
431 instead of 40% in control conditions, demonstrating the phagocytosis-inhibition ability of
432 secreted products. A similar significant trend was obtained at 4-6h after contact while 12/056
433 M24T1 ECPs had no effect on phagocytosis. The decrease of phagocytosis may be a
434 consequence of a loss of pseudopodia and reduction of adhesion capacity. This is reminiscent
435 of cell detachments and unspreadings frequently described for bivalve hemocytes challenged
436 with pathogenic *Vibrio* strains or with their extracellular products. For example, adhesion and
437 phagocytic activity of pacific oyster hemocytes were altered in contact with *V. aestuarianus*

438 01/32 ECPs or *V. tubiashii* 07/118 T2 ECPs (Labreuche et al., 2006; Mersni-Achour et al.,
439 2014) in a manner that was dependent on ECPs doses (Labreuche et al., 2006). The same
440 hemocyte responses were reported for *Mytilus edulis* and *Mya arenaria* hemocytes challenged
441 with the oyster pathogen *V. splendidus* LGP32 (Araya et al., 2009; Tanguy et al., 2013).
442 Nevertheless, precise molecular mechanisms involved in bacteria alteration of hemocyte
443 phagocytosis are still unclear. Involvement of metalloprotease activities have been suggested
444 since such enzymes are present in ECPs of virulent *Vibrios* and since the metalloenzyme
445 Vsm, secreted by *V. splendidus* LGP32 is toxic to oysters (Binesse et al., 2008). So, it will be
446 interesting to explore the effect of 10/068 1T1 ECPs on adult mussel.

447 Direct hemocyte phagocytosis of virulent and non virulent GFP-tagged bacteria was also
448 quantitatively investigated. The number of hemocytes strictly containing one engulfed *Vibrio*
449 decreased with time. This number was lower for cells exposed to the virulent strain 10/068
450 1T1 than for hemocytes incubated with the innocuous strain 12/056 M24T1. In appearance,
451 this result may suggest a more efficient destruction of *Vibrio* 10/068 1T1. Interestingly
452 however, analysis of hemocytes containing 2 or more *Vibrios* results in opposite findings. The
453 percentage hemocytes with 2 or more engulfed bacteria increased time-dependently but was
454 higher for the virulent strain. This latest observation is rather consistent with a faster
455 internalization of the pathogenic 10/068 1T1 strain in hemocytes, compared to 12/056
456 M24T1.

457 In some extent, internalization by host cells may be advantageous for invaders to
458 effectively establish infection and to colonize tissues (Sarantis and Grinstein, 2012). Such
459 mechanisms were observed in some *Vibrio* species, usually considered as extracellular
460 pathogens but having obviously intracellular stages (Duperthuy et al., 2011). This is
461 especially the case of, the coral pathogen *V. shiloi* which invades epithelial cells (Banin et
462 al., 2000) and of *V. splendidus* LGP32, able to attach and invade oyster hemocytes through
463 OmpU porin (Duperthuy et al., 2011). In a good agreement with these studies, it can be
464 proposed that the virulent strain 10/068 1T1 invades mussel hemocytes actively, although its
465 interaction with the cell inner environment remain to be determined.

466 Among the events taking place during the immune response, the oxidative burst plays an
467 important role in microbe destruction. ROS are lethal weapons used by phagocytes to kill
468 microbial invaders, directly, by causing oxidative damage to biocompounds, or indirectly, by
469 stimulating pathogen elimination (Paiva and Bozza, 2014). In *Mytilus edulis*, we confirmed
470 the capacity of hemocyte to produce oxygen radicals after stimulation by PMA at low doses
471 (García-García et al., 2008). When exposed to non virulent bacteria, mussel blood cells also

472 produced ROS at levels equivalent to the PMA treated group, 12/056 M24T1 ECPs also
473 enhanced oxidative bursts. Increases of ROS production by hemocytes exposed to bacteria or
474 to their extracellular products have been previously reported in the blue mussel (Tanguy et al.,
475 2013) and other bivalves species (Buggé et al., 2007; Lambert et al., 2003).

476 In the presence of virulent bacteria or of their ECPs, but not after hemocyte exposure to
477 heat killed virulent bacteria, ROS production was significantly inhibited by comparison to
478 PMA-stimulated levels. These data reveal the capacity of the pathogenic *V. splendidus*-related
479 strain 10/068 1T1 to alter cell activation by itself but also through secreted products. As a
480 consequence, it is possible that the pathogenic bacterial strain 10/068 1T1 actually quenches
481 ROS production in *M. edulis* hemocytes as a mean to survive within host cells. In this respect,
482 a wide variety of microbes have developed strategies to promote their survival within hostile
483 cellular environment, in particular by inhibition of ROS-mediated host responses (Spooner
484 and Yilmaz, 2011). For example Densmore et al. (1998) have demonstrated an inhibition of
485 oxidative burst in trout phagocytes, previously stimulated by PMA in the presence of *R.*
486 *salmoninarum* ECPs. In invertebrates, *L. anguillarum* does not induce any oxidative burst in
487 *Crassostrea virginica* hemocytes (Bramble and Anderson, 1997) and quenches ROS
488 production in lobster hemocytes (Moss and Allam, 2006). Likewise, the pathogenic strain *V.*
489 *harveyi* does not elicit ROS production when added to shrimp hemocytes contrary to a
490 probiotic strain of *V. alginolyticus* which induces cell activation (Muñoz et al., 2000). In
491 addition, *V. splendidus* LGP32 exhibits intracellular survival capabilities and escape from host
492 cellular defenses by avoiding acidic vacuole formation and by limiting ROS production
493 (Duperthuy et al., 2011).

494 5. Conclusion

495 In this study, we selected two *V. splendidus*-related strains and constructed GFP-tagged
496 models. The 10/068 1T1 strain was isolated from mortality events reported by professionals
497 and proven as virulent to blue mussel. The 12/056 M24T1 strain was isolated from normal
498 flora and found as innocuous. Functional immune responses of hemocytes challenged by
499 different strains were explored through cell motility, phagocytosis and oxidative burst.
500 Virulent bacteria generated stronger immunocyte responses. Overall, 10/068 1T1 enhanced
501 instantaneously cell migration but adversely affected cell motility after 2 hours exposures.
502 These bacteria were also able to quench ROS production and to alter phagocytosis capacity
503 through ECPs secretion. It has been shown that virulent bacteria were rapidly internalized by
504 hemocytes, suggesting more the involvement of a pathogen-controlled invasion strategy than

505 an immune cell-driven phagocytosis process. Taken together, our data support the hypothesis
506 that some bivalve pathogens escape cellular immune response by dysregulation of some
507 hemocyte bactericidal activities. Further investigations are necessary to establish whether
508 hemocytes also constitute carriers for tissues infection.

509

510 **Acknowledgements**

511 This work received fundings from the State/Region Plan Contract (CPER) allocated through
512 the Research Federation FED 4116 SCALE (Sciences Appliquées à L'Environnement),),
513 from the FP7-European project BIVALIFE 'Controlling infectious diseases in oysters and
514 mussels in Europe' (Grant Agreement 266157) and DGAI support through National Reference
515 Laboratory activities for mollusk diseases (Ifremer-La Tremblade). Yosra Ben Cheikh was a
516 recipient for a Ph.D. grant from the Conseil Regional de Haute-Normandie. The authors are
517 indebted to the marine fish farm Aquacaux (Octeville, France) for valuable technical
518 assistance. Dr. Eric Stabb (Dept. Microbiology, University of Georgia, Athens, USA) is
519 kindly acknowledged for providing us with his excellent *Vibrio* vectors and helper strain. We
520 also thanks LGPMM technical unit, Manon Garrigues and Philippe Haffner for their
521 contribution.

522

523 **Supplementary data**

524 **Video 1:** Epifluorescence time-lapse microscopy of hemocytes plated in a culture dish and co-
525 incubated at 15°C with the 10/068 1T1 *Vibrio* strain. Nuclei were stained with a vital DNA
526 dye Hoechst 33342 (5µM). Recording time, 2 hours. Imaging interval time, 30 sec.

527 **References**

528 Aboubaker, M.H., Sabrié, J., Huet, M., Koken, M., 2013. Establishment of stable GFP-tagged
529 *Vibrio aestuarianus* strains for the analysis of bacterial infection-dynamics in the Pacific
530 oyster, *Crassostrea gigas*. Vet. Microbiol. 164, 392–398.

531 Allison, D.G., Sattenstall, M.A., 2007. The influence of green fluorescent protein
532 incorporation on bacterial physiology: a note of caution. J. Appl. Microbiol. 103, 318–324.

533 Alvarez, M.R., Friedl, F.E., Roman, F.R., 1995. *In vivo* chemoactivation of oyster hemocytes
534 induced by bacterial secretion products. J. Invertebr. Pathol. 66, 287–292.

- 535 Araya, M.T., Siah, A., Mateo, D.R., Markham, F., McKenna, P., Johnson, G.R., Berthe,
536 F.C.J., 2009. Morphological and molecular effects of *Vibrio splendidus* on hemocytes of
537 softshell clams, *Mya arenaria*. Journal of Shellfish Research 28, 751–758.
- 538 Balbi, T., Fabbri, R., Cortese, K., Smerilli, A., Ciacci, C., Grande, C., Vezzulli, L., Pruzzo, C.,
539 Canesi, L., 2013. Interactions between *Mytilus galloprovincialis* hemocytes and the bivalve
540 pathogens *Vibrio aestuarianus* 01/032 and *Vibrio splendidus* LGP32. Fish Shellfish Immunol.
541 35, 1906–1915.
- 542 Banin, E., Israely, T., Kushmaro, A., Loya, Y., Orr, E., Rosenberg, E., 2000. Penetration of
543 the coral-bleaching bacterium *Vibrio shiloi* into *Oculina patagonica*. Appl Environ Microbiol
544 66, 3031–3036.
- 545 Bayne, C.J., 1990. Phagocytosis and non-self recognition in invertebrates phagocytosis
546 appears to be an ancient line of defense. BioScience 40, 723–731.
- 547 Beaz-Hidalgo, R., Balboa, S., Romalde, J.L., Figueras, M.J., 2010a. Diversity and
548 pathogenicity of *Vibrio* species in cultured bivalve molluscs. Environ Microbiol Rep 2, 34–
549 43.
- 550 Beaz-Hidalgo, R., Diéguez, A.L., Cleenwerck, I., Balboa, S., Doce, A., de Vos, P., Romalde,
551 J.L., 2010b. *Vibrio celticus* sp. nov., a new *Vibrio* species belonging to the *Splendidus* clade
552 with pathogenic potential for clams. Syst. Appl. Microbiol. 33, 311–315.
- 553 Bechemin, C., Soletchnik, P., Polsenaere, P., Le Moine, O., Pernet, F., Protat, M., Fuhrmann,
554 M., Quere, C., Goulitquer, S., Corporeau, C., Renault, T., Lapegue, S., Travers, M.-A.,
555 Morga, B., Garriques, M., Garcia, C., Haffner, P., Dubreuil, C., Faury, N., Baillon, L., Baud,
556 J.-P., 2014. Surmortalités de la moule bleue *Mytilus edulis* dans les Pertuis Charentais (mars
557 2014).
- 558 Binesse, J., Delsert, C., Saulnier, D., Champomier-Vergès, M.-C., Zagorec, M., Munier-
559 Lehmann, H., Mazel, D., Le Roux, F., 2008. Metalloprotease vsm is the major determinant of
560 toxicity for extracellular products of *Vibrio splendidus*. Appl. Environ. Microbiol. 74, 7108–
561 7117.
- 562 Bramble, L., Anderson, R.S., 1997. Modulation of *Crassostrea virginica* hemocyte reactive
563 oxygen species production by *Listonella anguillarum*. Dev. Comp. Immunol. 21, 337–348.
- 564 Buggé, D.M., Hégaret, H., Wikfors, G.H., Allam, B., 2007. Oxidative burst in hard clam
565 (*Mercenaria mercenaria*) haemocytes. Fish Shellfish Immunol. 23, 188–196.
- 566 Canesi, L., Gallo, G., Gavioli, M., Pruzzo, C., 2002. Bacteria-hemocyte interactions and
567 phagocytosis in marine bivalves. Microsc. Res. Tech. 57, 469–476.
- 568 Casadevall, A., Pirofski, L.-A., 2009. Virulence factors and their mechanisms of action: the
569 view from a damage-response framework. J Water Health 7 Suppl 1, S2–S18.

- 570 Ciacci, C., Betti, M., Canonico, B., Citterio, B., Roch, P., Canesi, L., 2010. Specificity of anti-
571 *Vibrio* immune response through p38 MAPK and PKC activation in the hemocytes of the
572 mussel *Mytilus galloprovincialis*. *J. Invertebr. Pathol.* 105, 49–55.
- 573 Ciacci, C., Citterio, B., Betti, M., Canonico, B., Roch, P., Canesi, L., 2009. Functional
574 differential immune responses of *Mytilus galloprovincialis* to bacterial challenge. *Comp.*
575 *Biochem. Physiol. B, Biochem. Mol. Biol.* 153, 365–371.
- 576 Costa, M.M., Prado-Alvarez, M., Gestal, C., Li, H., Roch, P., Novoa, B., Figueras, A., 2009.
577 Functional and molecular immune response of Mediterranean mussel (*Mytilus*
578 *galloprovincialis*) haemocytes against pathogen-associated molecular patterns and bacteria.
579 *Fish Shellfish Immunol.* 26, 515–523.
- 580 Densmore, C.L., Smith, S.A., Holladay, S.D., 1998. *In vitro* effects of the extracellular protein
581 of *Renibacterium salmoninarum* on phagocyte function in brook trout (*Salvelinus fontinalis*).
582 *Vet. Immunol. Immunopathol.* 62, 349–357.
- 583 Donaghy, L., Lambert, C., Choi, K.-S., Soudant, P., 2009. Hemocytes of the carpet shell clam
584 (*Ruditapes decussatus*) and the Manila clam (*Ruditapes philippinarum*): Current knowledge
585 and future prospects. *Aquaculture* 297, 10–24.
- 586 Dunn, A.K., Millikan, D.S., Adin, D.M., Bose, J.L., Stabb, E.V., 2006. New rfp- and pES213-
587 derived tools for analyzing symbiotic *Vibrio fischeri* reveal patterns of infection and lux
588 expression *in situ*. *Appl. Environ. Microbiol.* 72, 802–810.
- 589 Duperthuy, M., Schmitt, P., Garzón, E., Caro, A., Rosa, R.D., Le Roux, F., Lautrédou-
590 Audouy, N., Got, P., Romestand, B., de Lorgeril, J., Kieffer-Jaquinod, S., Bachère, E.,
591 Destoumieux-Garzón, D., 2011. Use of OmpU porins for attachment and invasion of
592 *Crassostrea gigas* immune cells by the oyster pathogen *Vibrio splendidus*. *Proc. Natl. Acad.*
593 *Sci. U.S.A.* 108, 2993–2998.
- 594 Felsenstein, J., 1985. Confidence limits on phylogenies: An approach using the bootstrap.
595 *evolution* 39, 783–791.
- 596 García-García, E., Prado-Alvarez, M., Novoa, B., Figueras, A., Rosales, C., 2008. Immune
597 responses of mussel hemocyte subpopulations are differentially regulated by enzymes of the
598 PI 3-K, PKC, and ERK kinase families. *Dev. Comp. Immunol.* 32, 637–653.
- 599 Gay, M., Renault, T., Pons, A.-M., Le Roux, F., 2004. Two *Vibrio splendidus* related strains
600 collaborate to kill *Crassostrea gigas*: taxonomy and host alterations. *Dis. Aquat. Org.* 62, 65–
601 74.
- 602 Gestal, C., Roch, P., Renault, T., Pallavicini, A., Paillard, C., Novoa, B., Oubella, R., Venier,
603 P., Figueras, A., 2008. Study of diseases and the immune system of bivalves using molecular
604 biology and genomics. *Reviews in Fisheries Science* 16, 133–156.
- 605 Gosling, E., 2015. Marine bivalve molluscs. John Wiley & Sons.

- 606 Guichard, B., Francois, C., Joly, J.-P., Garcia, C., Saulnier, D., Pepin, J.-F., Arzul, I., Omnes,
607 E., Tourbiez, D., Faury, N., Haffner, P., Chollet, B., Robert, M., Renault, T., Rauflet, F., Le
608 Gagneur, E., Ropert, M., Mouillard, G., Gerla, D., Annezo, J.-P., Le Gal, D., Langlade, A.,
609 Bedier, E., Brerette, S., Chabirand, J.-M., Grizon, J., Robert, S., Courtois, O., Rumebe, M.,
610 Cantin, C., 2011. Bilan 2010 du réseau Repamo - Réseau national de surveillance de la santé
611 des mollusques marins.
- 612 Hunt, D.E., David, L.A., Gevers, D., Preheim, S.P., Alm, E.J., Polz, M.F., 2008. Resource
613 partitioning and sympatric differentiation among closely related bacterioplankton. *Science*
614 320, 1081–1085.
- 615 Kesarcodi-Watson, A., Kaspar, H., Lategan, M.J., Gibson, L., 2009. Two pathogens of
616 Greenshell mussel larvae, *Perna canaliculus*: *Vibrio splendidus* and a *V.*
617 *coralliilyticus/neptunius*-like isolate. *J. Fish Dis.* 32, 499–507.
- 618 Knodler, L.A., Bestor, A., Ma, C., Hansen-Wester, I., Hensel, M., Vallance, B.A., Steele-
619 Mortimer, O., 2005. Cloning vectors and fluorescent proteins can significantly inhibit
620 *Salmonella enterica* virulence in both epithelial cells and macrophages: implications for
621 bacterial pathogenesis studies. *Infect. Immun.* 73, 7027–7031.
- 622 Kwan, T.N., Bolch, C.J.S., 2015. Genetic diversity of culturable *Vibrio* in an Australian blue
623 mussel *Mytilus galloprovincialis* hatchery. *Dis. Aquat. Org.* 116, 37–46.
- 624 Labreuche, Y., Le Roux, F., Henry, J., Zatylny, C., Huvet, A., Lambert, C., Soudant, P.,
625 Mazel, D., Nicolas, J.-L., 2010. *Vibrio aestuarianus* zinc metalloprotease causes lethality in
626 the Pacific oyster *Crassostrea gigas* and impairs the host cellular immune defenses. *Fish*
627 *Shellfish Immunol.* 29, 753–758.
- 628 Labreuche, Y., Soudant, P., Gonçalves, M., Lambert, C., Nicolas, J.-L., 2006. Effects of
629 extracellular products from the pathogenic *Vibrio aestuarianus* strain 01/32 on lethality and
630 cellular immune responses of the oyster *Crassostrea gigas*. *Dev. Comp. Immunol.* 30, 367–
631 379.
- 632 Lacoste, A., Jalabert, F., Malham, S., Cueff, A., Gélébart, F., Cordevant, C., Lange, M.,
633 Poulet, S.A., 2001. A *Vibrio splendidus* strain is associated with summer mortality of juvenile
634 oysters *Crassostrea gigas* in the Bay of Morlaix (North Brittany, France). *Dis. Aquat. Org.*
635 46, 139–145.
- 636 Lambert, C., Nicolas, J.L., Cilia, V., 1999. *Vibrio splendidus*-related strain isolated from
637 brown deposit in scallop (*pecten maximus*) cultured in Brittany (France). *Bull. Eur. Ass.*
638 *Fish Pathol.* 102.
- 639 Lambert, C., Soudant, P., Choquet, G., Paillard, C., 2003. Measurement of *Crassostrea gigas*
640 hemocyte oxidative metabolism by flow cytometry and the inhibiting capacity of pathogenic
641 *Vibrios*. *Fish Shellfish Immunol.* 15, 225–240.

- 642 Le Foll, F., Rioult, D., Boussa, S., Pasquier, J., Dagher, Z., Leboulenger, F., 2010.
643 Characterisation of *Mytilus edulis* hemocyte subpopulations by single cell time-lapse motility
644 imaging. Fish Shellfish Immunol. 28, 372–386.
- 645 Le Roux, F., Gay, M., Lambert, C., Nicolas, J.L., Gouy, M., Berthe, F., 2004. Phylogenetic
646 study and identification of *Vibrio splendidus*-related strains based on *gyrB* gene sequences.
647 Dis. Aquat. Org. 58, 143–150.
- 648 Liu, D.-W., 2008. Opioid peptides and innate immune response in mollusc. Protein Pept. Lett.
649 15, 683–686.
- 650 Mersni-Achour, R., Imbert-Auvray, N., Huet, V., Ben Cheikh, Y., Faury, N., Doghri, I.,
651 Rouatbi, S., Bordenave, S., Travers, M.-A., Saulnier, D., Fruitier-Arnaudin, I., 2014. First
652 description of French *V. tubiashii* strains pathogenic to mollusk: II. Characterization of
653 properties of the proteolytic fraction of extracellular products. J. Invertebr. Pathol. 123, 49–
654 59.
- 655 Mitta, G., Vandenbulcke, F., Roch, P., 2000. Original involvement of antimicrobial peptides
656 in mussel innate immunity. FEBS Lett. 486, 185–190.
- 657 Moss, B., Allam, B., 2006. Fluorometric measurement of oxidative burst in lobster hemocytes
658 and inhibiting effect of pathogenic bacteria and hypoxia. Journal of Shellfish Research 25,
659 1051–1057.
- 660 Muñoz, M., Cedeño, R., Rodríguez, J., van der Knaap, W.P.W., Mialhe, E., Bachère, E.,
661 2000. Measurement of reactive oxygen intermediate production in haemocytes of the penaeid
662 shrimp, *Penaeus vannamei*. Aquaculture 191, 89–107.
- 663 Paiva, C.N., Bozza, M.T., 2014. Are reactive oxygen species always detrimental to
664 pathogens? Antioxid. Redox Signal. 20, 1000–1037.
- 665 Parisi, M.-G., Li, H., Jouvét, L.B.P., Dyrzynda, E.A., Parrinello, N., Cammarata, M., Roch, P.,
666 2008. Differential involvement of mussel hemocyte sub-populations in the clearance of
667 bacteria. Fish Shellfish Immunol. 25, 834–840.
- 668 Pruzzo, C., Gallo, G., Canesi, L., 2005. Persistence of *Vibriosis* in marine bivalves: the role of
669 interactions with haemolymph components. Environ. Microbiol. 7, 761–772.
- 670 Rioult, D., Lebel, J.-M., Le Foll, F., 2013. Cell tracking and velocimetric parameters analysis
671 as an approach to assess activity of mussel (*Mytilus edulis*) hemocytes *in vitro*.
672 Cytotechnology 65, 749–758.
- 673 Rioult, D., Pasquier, J., Boulangé-Lecomte, C., Poret, A., Abbas, I., Marin, M., Minier, C., Le
674 Foll, F., 2014. The multi-xenobiotic resistance (MXR) efflux activity in hemocytes of *Mytilus*
675 *edulis* is mediated by an ATP binding cassette transporter of class C (ABCC) principally
676 inducible in eosinophilic granulocytes. Aquat. Toxicol. 153, 98–109.
- 677 Russell, D.G., 2001. Phagocytosis, in: eLS. John Wiley & Sons, Ltd.

- 678 Saitou, N., Nei, M., 1987. The neighbor-joining method: a new method for reconstructing
679 phylogenetic trees. *Mol. Biol. Evol.* 4, 406–425.
- 680 Sarantis, H., Grinstein, S., 2012. Subversion of phagocytosis for pathogen survival. *Cell Host*
681 *Microbe* 12, 419–431.
- 682 Saulnier, D., De Decker, S., Haffner, P., 2009. Real-time PCR assay for rapid detection and
683 quantification of *Vibrio aestuarianus* in oyster and seawater: a useful tool for epidemiologic
684 studies. *J. Microbiol. Methods* 77, 191–197.
- 685 Saulnier, D., De Decker, S., Haffner, P., Cobret, L., Robert, M., Garcia, C., 2010. A large-
686 scale epidemiological study to identify bacteria pathogenic to Pacific oyster *Crassostrea gigas*
687 and correlation between virulence and metalloprotease-like activity. *Microb. Ecol.* 59, 787–
688 798.
- 689 Schneeweiss, H., Renwantz, L., 1993. Analysis of the attraction of haemocytes from *Mytilus*
690 *edulis* by molecules of bacterial origin. *Dev. Comp. Immunol.* 17, 377–387.
- 691 Nicolas, J.L., Corre, S., Gauthier, G., Robert, R., Ansquer, D., 1996. Bacterial problems
692 associated with scallop *Pecten maximus* larval culture. *Diseases of Aquatic Organisms -*
693 *Disease Aquat Org* 27, 67–76.
- 694 Spooner, R., Yilmaz, Ö., 2011. The role of Reactive-Oxygen-Species in microbial persistence
695 and inflammation. *Int J Mol Sci* 12, 334–352.
- 696 Stabb, E.V., Ruby, E.G., 2002. RP4-based plasmids for conjugation between *Escherichia coli*
697 and members of the *Vibrionaceae*. *Meth. Enzymol.* 358, 413–426.
- 698 Steinhaus, Edward Arthur, Martignoni, Mauro E., 1970. An abridged glossary of terms used
699 in invertebrate pathology
- 700 Tanguy, M., McKenna, P., Gauthier-Clerc, S., Pellerin, J., Danger, J.-M., Siah, A., 2013.
701 Functional and molecular responses in *Mytilus edulis* hemocytes exposed to bacteria, *Vibrio*
702 *splendidus*. *Dev. Comp. Immunol.* 39, 419–429.
- 703 Thompson, F.L., Gevers, D., Thompson, C.C., Dawyndt, P., Naser, S., Hoste, B., Munn, C.B.,
704 Swings, J., 2005. Phylogeny and molecular identification of *Vibriosis* on the basis of multilocus
705 sequence analysis. *Appl. Environ. Microbiol.* 71, 5107–5115.
- 706 Travers, M.-A., Boettcher Miller, K., Roque, A., Friedman, C.S., 2015. Bacterial diseases in
707 marine bivalves. *Journal of Invertebrate Pathology*.
- 708 Watermann, B.T., Herlyn, M., Daehne, B., Bergmann, S., Meemken, M., Kolodzey, H., 2008.
709 Pathology and mass mortality of Pacific oysters, *Crassostrea gigas* (Thunberg), in 2005 at the
710 East Frisian coast, Germany. *J. Fish Dis.* 31, 621–630.

711

712

713

714 **Figure legends**

715 **Figure 1.** Cumulative mortalities recorded after experimental bacterial infections of adult
716 mussels. Bacterial strains were grown for 24 h in Marine broth before resuspension into
717 filtered sterile seawater (FSSW) and adjustment to $OD_{600} = 1$. One hundred microliters of
718 bacterial suspension were injected intramuscularly to anesthetized mussels (10
719 animals/replicate). Mussels injected with FSSW were used as control. Data are means \pm SEM
720 of cumulative mortalities triplicate tanks

721

722 **Figure 2.** Effect of inoculum size on mussel mortality. Dose-response effect of *V. splendidus*-
723 related strain 10/068 1T1 on adult mussels estimated 24 hours post-injection. Mussels injected
724 with FSSW were used as control. Data are means \pm SEM of triplicate tanks.

725

726 **Figure 3.** Phylogenetic analysis of bacteria strains based on *gyrB* gene sequencing.
727 The percentage of replicate trees in which the associated taxa clustered together in the
728 bootstrap test (1000 replicates) are shown next to the branches. The analysis was carried out
729 by the neighbor-joining method on 34 nucleotide sequences and 529 positions in the final
730 dataset. Evolutionary analyses were conducted in MEGA6. Virulence of bacteria, assessed by
731 the percentage of mortality induced 24 hours post-injection is indicated by the horizontal bars.

732

733 **Figure 4.** Plasmid expression stability in *Vibrio* strains and effect of GFP expression on
734 growth capacities and virulence. (a) Fluorescence conservation in GFP-tagged bacteria over
735 time. Strains were cultivated in non-selective LBS medium and fluorescence was estimated by
736 flow cytometry. (b) Growth curve of parental and GFP-tagged bacteria at 22°C in LBS
737 medium ($n=3 \pm$ SEM). (c) Comparison of virulence capacity of parental and GFP-tagged
738 strains on adult mussels ($n=3 \pm$ SEM).

739

740 **Figure 5.** Effect of *V. splendidus*-related strains on hemocyte motility. *M. edulis* hemocytes
741 were challenged by *V. splendidus*-related strains 10/068 1T1 or 12/056 M24T1 at 10^8 cfu.ml⁻¹
742 or incubated in MPSS (control) during 2h at 15°C. (a) Mean velocity of 60 nuclei (3
743 independents experiences) obtained from centroid XY coordinate changes in the microscopic

744 field between two successive images, separated by 30 seconds. (b) Standard errors of the
745 mean taken from (a).

746 **Figure 6.** Effect of bacterial ECPs on bead phagocytosis ability. (a) Flow cytometry analysis
747 of hemocyte incubated *in vitro* with latex beads during 2, 4 and 6 hours. The percentage of
748 cells containing 3 beads or more was measured (mean \pm SEM, n=6, p<0.05, Student's t-test).
749 (b) Phase contrast (Ph) and fluorescence (Fitc) microscopy observation of hemocytes after 2
750 hours phagocytosis (bar 10 μ m).

751
752 **Figure 7.** Hemocyte phagocytic ability towards GFP-tagged bacteria. (a) Comparison
753 between the internalization of virulent and non-virulent bacteria after *in vitro* exposure during
754 2, 4 and 6 hours. Left Y-axis and solid bars refer to the percentage of hemocytes containing 2
755 or more bacteria. Right Y-axis and dashed bars refer to the percentage of hemocytes
756 containing at least one *Vibrio*. Significant values respectively to non-virulent strain are
757 represented with *** (p<0.001, Student's t-test). Data are means \pm SEM, n=6. (b) Phase
758 contrast (Ph) and fluorescence (Fitc) microscopy observations of hemocyte after
759 internalization of *Vibrio* strains 10/068 1T1 or 12/056 M24T1, bar 10 μ m.

760
761 **Figure 8.** ROS production in *M. edulis* hemocytes. Hemocytes were pre-exposed 2 hours to
762 heat killed or living virulent bacteria at 10^8 cfu.ml⁻¹, non-virulent bacterial strain at 10^8 cfu.ml⁻¹
763 ¹, or their extracellular products or PMA 0,2 μ M. Cell fluorescence was quantified by flow
764 cytometry after incubation with CM-H₂DCFDA at 0.2 μ M f.c. Data are means of fluorescence
765 \pm SEM, A.U., n=6. * indicates significant differences from control (Mann-Whitney rank sum
766 test, p< 0.05) and § marks significant differences from PMA (Student's t-test § p<0.05, §§§
767 p<0.001.

768

769

770

Table 1. Strains used in this study

Strain	Isolation from	Context	Date
10/058 2T1	Mussel, baie de Somme (80) France	Mussel mortality	2010, May 18
10/058 3T1	Mussel, baie de Somme (80) France	Mussel mortality	2010, May 18
10/060 2T1	Mussel, baie d'Authie (62) France	Mussel mortality	2010, May 19
10/068 1T1	Mussel, baie de Camaret (29) France	Mussel mortality	2010, May 31
11/100 M22T3	Mussel, d'Agnas (17) France	Absence of mortality	2011, June 29
11/148 M6T2	Mussel, d'Agnas (17) France	Absence of mortality	2011, October 11
12/037 M22T1	Mussel, d'Agnas (17) France	Absence of mortality	2012, May 22
12/037 M23T1	Mussel, d'Agnas (17) France	Absence of mortality	2012, May 22
12/037 M24T1	Mussel, d'Agnas (17) France	Absence of mortality	2012, May 22
12/037 M7T1	Mussel, d'Agnas (17) France	Absence of mortality	2012, May 22
12/040 11T2	Mussel, Oye Plage (62) France	Mussel mortality	2012, May 24
12/056 M1T1	Mussel, d'Agnas (17) France	Absence of mortality	2012, June 05
12/056 M24T1	Mussel, d'Agnas (17) France	Absence of mortality	2012, June 05
13/026 2T3	Mussel, Oye Plage (62) France	Mussel mortality	2013, April 08
13/026 5T3	Mussel, Oye Plage (62) France	Mussel mortality	2013, April 08

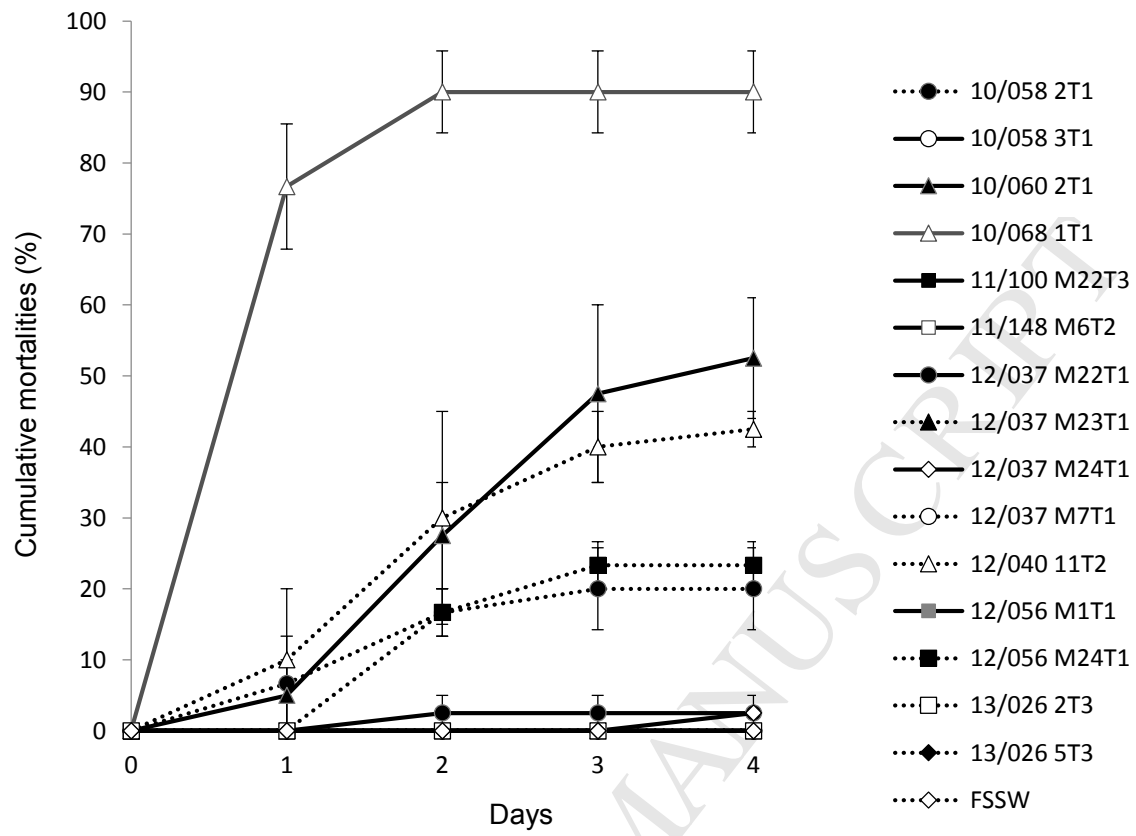
1 **Table 1.** Gyrase B gi reference

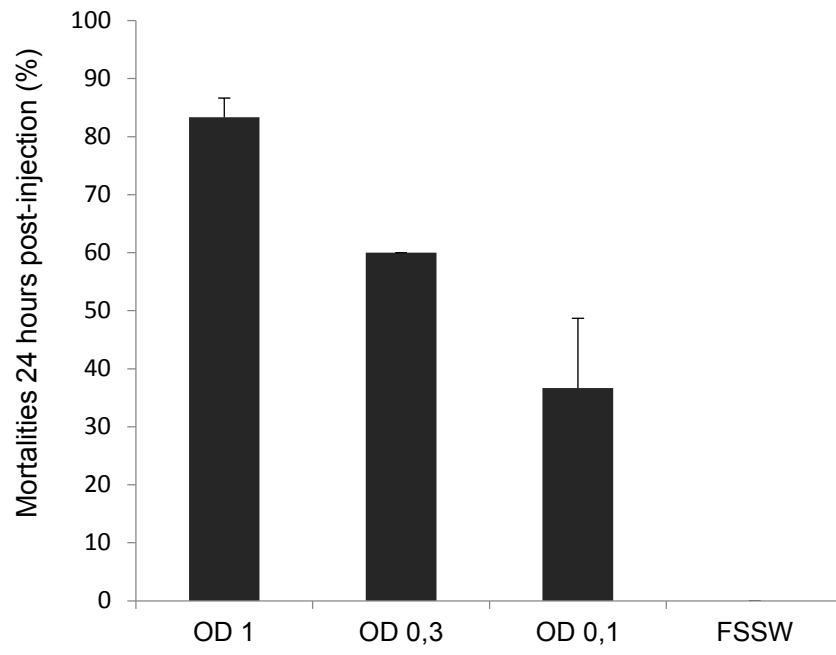
gi number	reference strains
gi 164456642	<i>Vibrio brasiliensis</i> strain LMG 20546T
gi 164456646	<i>Vibrio chagasii</i> strain LMG 21353T
gi 164456648	<i>Vibrio cholerae</i> strain IID 6019
gi 164456652	<i>Vibrio crassostreae</i> strain LMG 22240T
gi 164456656	<i>Vibrio cyclitrophicus</i> strain LMG 21359T
gi 164456666	<i>Vibrio fortis</i> strain LMG 21557T
gi 164456672	<i>Vibrio gigantis</i> strain LMG 22741T
gi 164456684	<i>Vibrio kanaloae</i> strain LMG 20539T
gi 164456686	<i>Vibrio lentus</i> strain LMG 21034T
gi 164456718	<i>Vibrio pomeroyi</i> strain LMG 20537T
gi 164456730	<i>Vibrio splendidus</i> strain LMG 19031T
gi 164456734	<i>Vibrio tasmaniensis</i> strain LMG 20012T
gi 164456742	<i>Vibrio xuii</i> strain LMG 21346T
gi 564274123	<i>Vibrio artabrorum</i> strain CAIM 1845 T
gi 564274125	<i>Vibrio atlanticus</i> strain CAIM 1847 T
gi 564274131	<i>Vibrio celticus</i> strain CAIM 1849 T
gi 754496442	<i>Vibrio gallaecicus</i> strain CECT 7244T
gi 564274143	<i>Vibrio toranzoniae</i> strain CAIM 1869 T
KU145472	10/058 2T1
KU145473	10/058 3T1
KU145474	10/060 2T1
KU145475	10/068 1T1
KU145476	11/100 M22T3
KU145477	11/148 M6T2
KU145478	12/037 M22T1
KU145479	12/037 M23T1
KU145480	12/037 M24T1

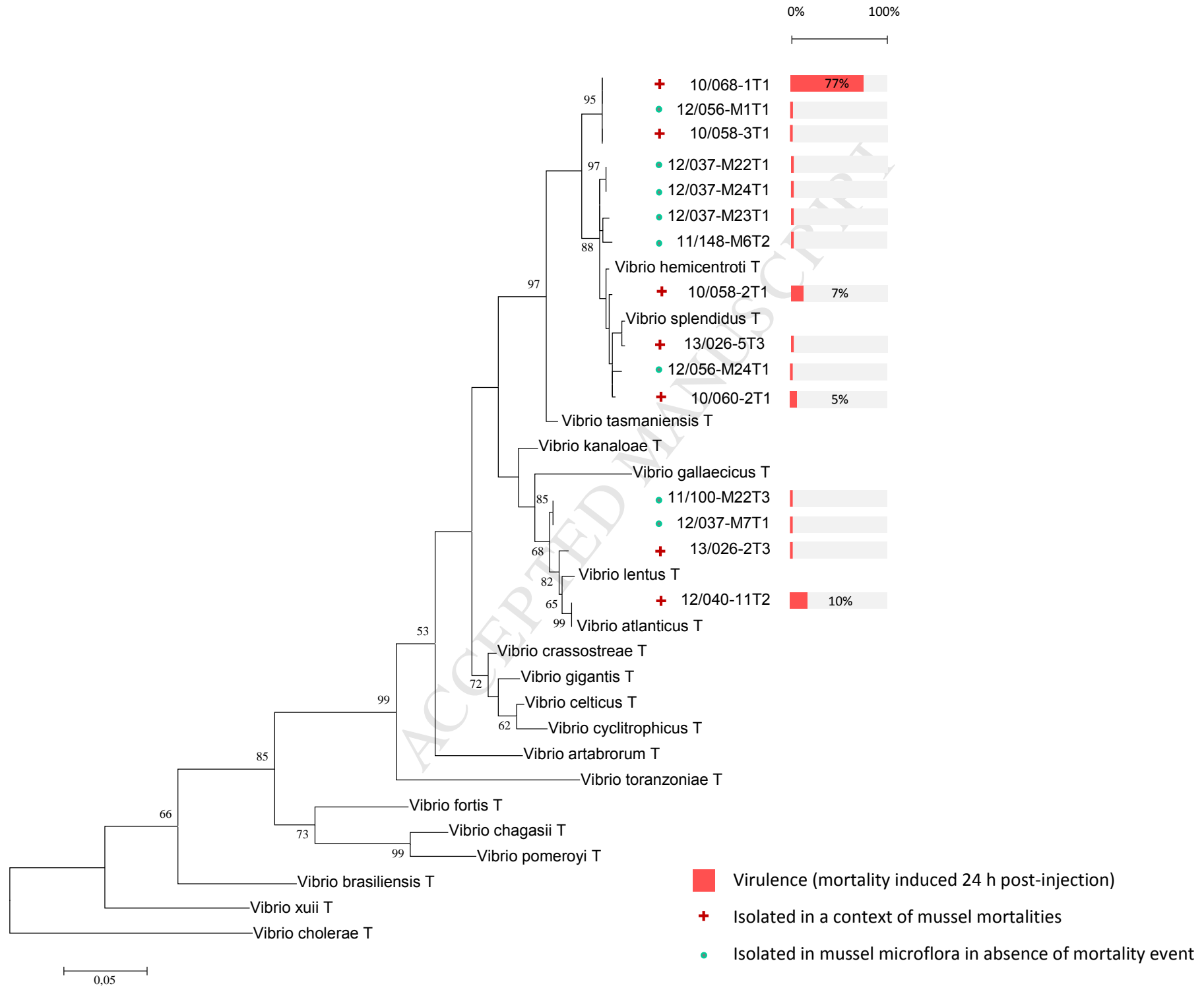
KU145481	12/037 M7T1
KU145482	12/040 11T2
KU145483	12/056 M1T1
KU145486	12/056 M24T1
KU145484	13/026 2T3
KU145485	13/026 5T3

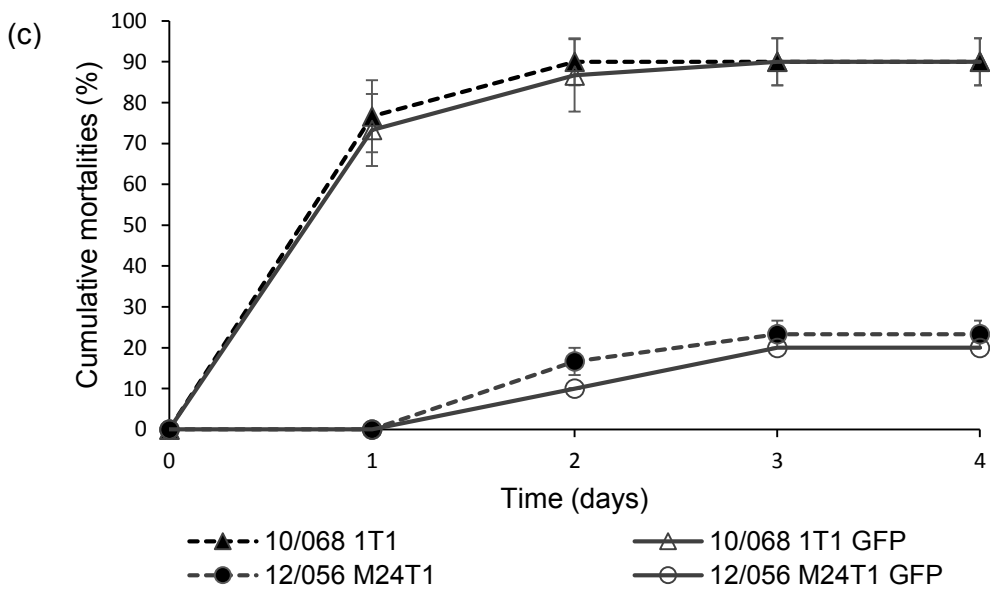
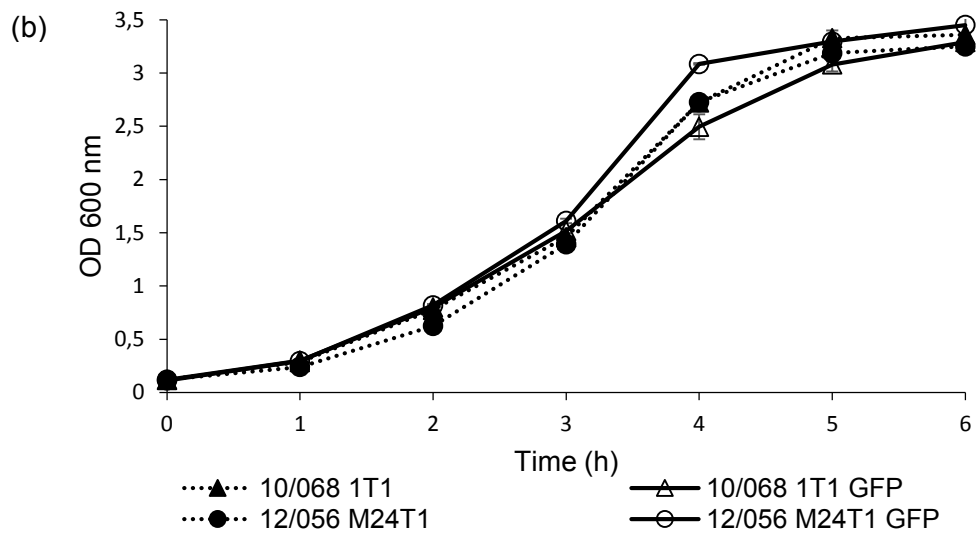
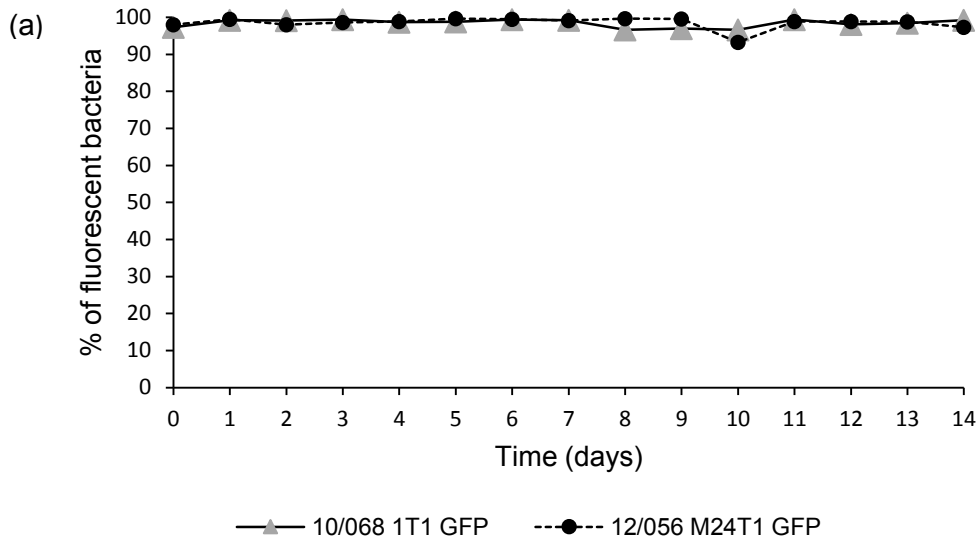
2

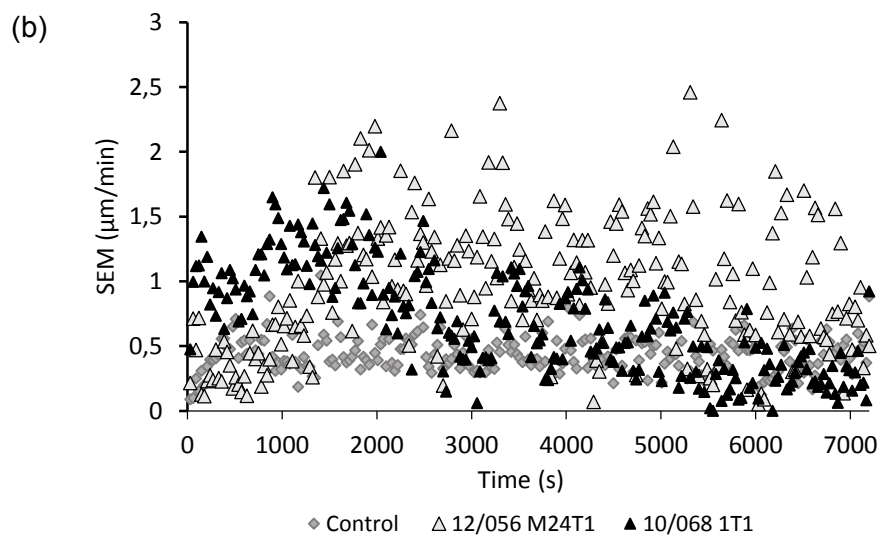
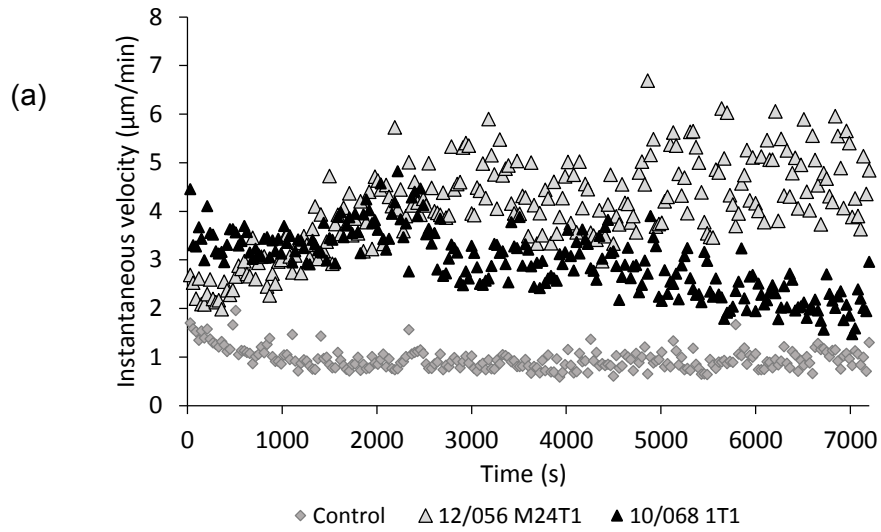
3



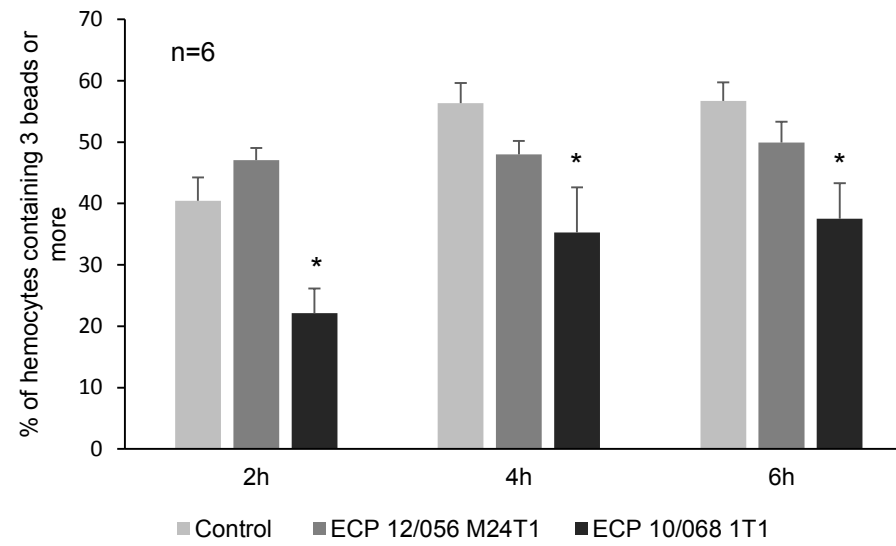




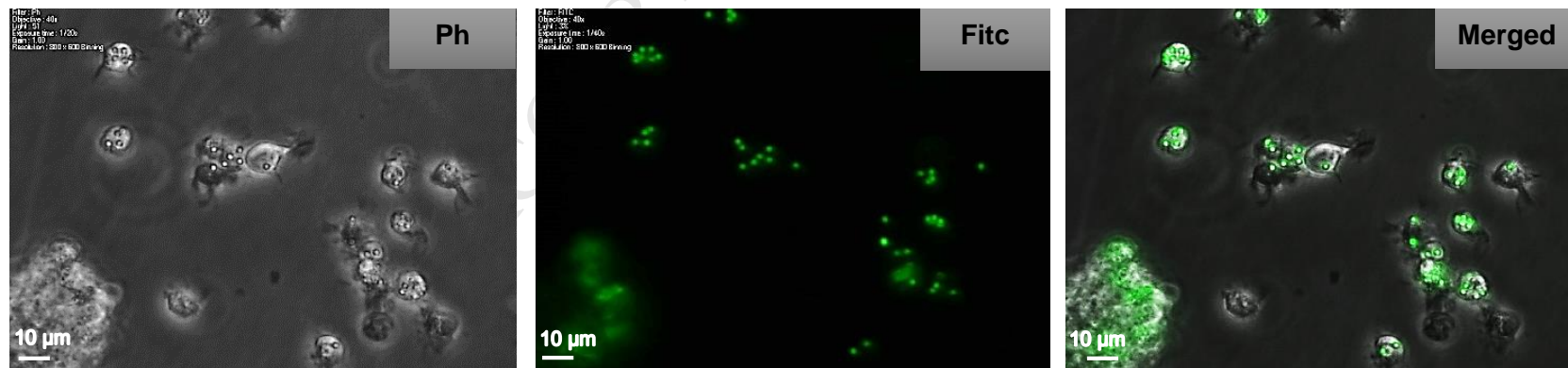


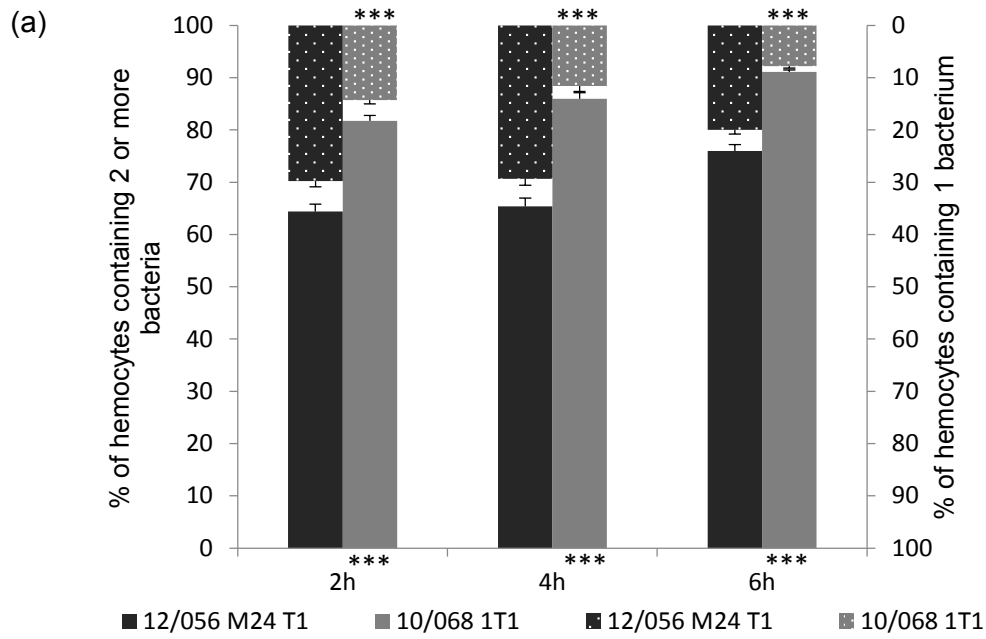


(a)



(b)





(b)

